SUPPLEMENTARY INFORMATION

Pericytes impair capillary blood flow and motor function after chronic spinal cord injury.

Yaqing Li[1], Ana M. Lucas-Osma[1], Sophie Black[1], Mischa V. Bandet[2], Marilee J. Stephens[1], Romana Vavrek[1], Leo Sanelli[1], Keith K. Fenrich[1], Antonio F. Di Narzo[3], Stella Dracheva[4,5], Ian R. Winship[2], Karim Fouad[1] and David J. Bennett[1]

[1]Neuroscience and Mental Health Institute and Faculty of Rehabilitation Medicine, University of Alberta, Canada; [2]Neuroscience and Mental Health Institute and Department of Psychiatry, University of Alberta, Canada; [3]Department of Genetics and Genomic Sciences and [4]The Friedman Brain Institute, Icahn School of Medicine at Mount Sinai, New York, NY, USA; [5]James J. Peters VA Medical Center, Bronx, NY, USA

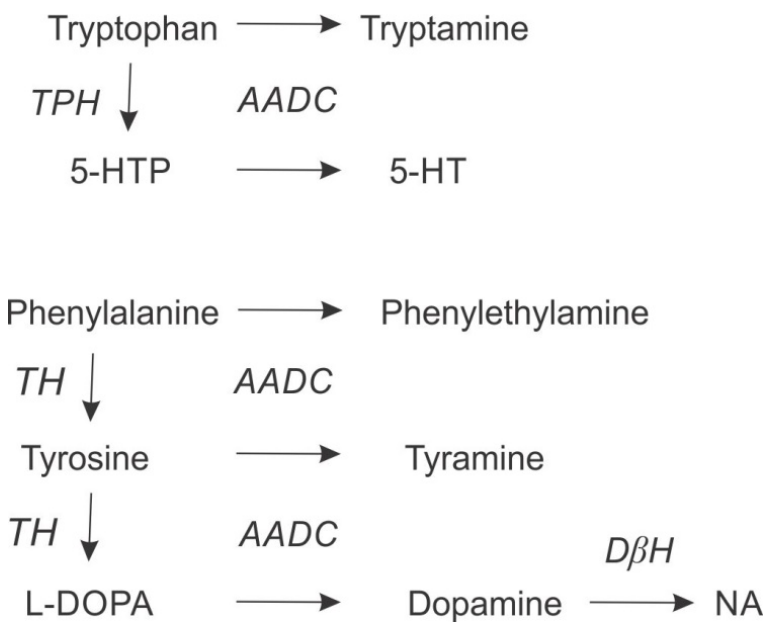

Supplementary Figure 1. Amine synthesis pathways. Amino acids are directly converted by aromatic-L-amino-acid-decarboxylase (*AADC)* to trace amines (tryptamine, phenylethylamine and tyramine). Amino acids are also hydroxylated by tryptophan hydroxylase (*TPH*) and tyrosine hydroxylase (*TH*) to form the monoamine precursors 5-hydroxytryptamine (5-HTP) and L-DOPA, which are then converted by *AADC* to 5-HT and dopamine. Dopamine beta-hydroxylase (*DβH*) then converts dopamine to NA. Monoamine oxidase (*MAO*) metabolizes all these amines (not shown). Enzymes in italics.

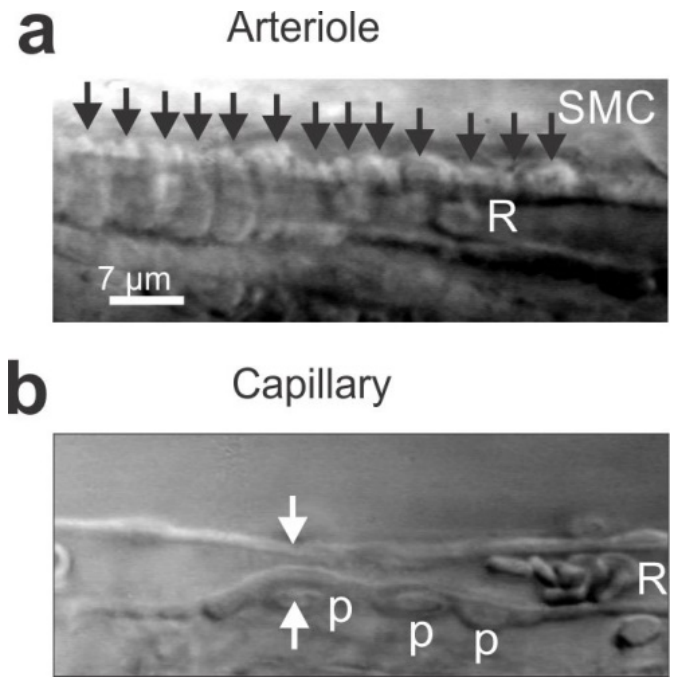

Supplementary Figure 2. Identification of spinal cord arterioles and capillaries in chronic spinal rats. Vessels from S4 sacral spinal cord maintained *in vitro* and imaged with IR DIC microscopy. **(a)** Arteriole continuously covered with smooth muscle cells (SMCs, one cell per black arrow), with a few red blood cells inside (R). The vessel angles out of the plane of focus toward the right, allowing the surface of SMCs to be viewed on left and centre of vessel viewed on right (at R), with SMCs seen in cross section on vessel wall. **(b)** Capillary connected to arteriole in **a**. This capillary is devoid of SMCs, and instead pericytes (p) sparsely cover the capillary. This capillary has a spontaneous constriction at the pericytes indicated by the white arrows. Such spontaneous constrictions occurred near regions where the capillary was damaged nearby during cord removal for *in vitro* recording (500 µm to left of capillary; not shown). Such damaged capillaries were not used in our analysis of pericyte actions with trace amines, and is shown here simply to illustrate how pericytes are distinguished from SMCs, and serve as sphincters, rather than constricting the entire vessel, as SMCs do.

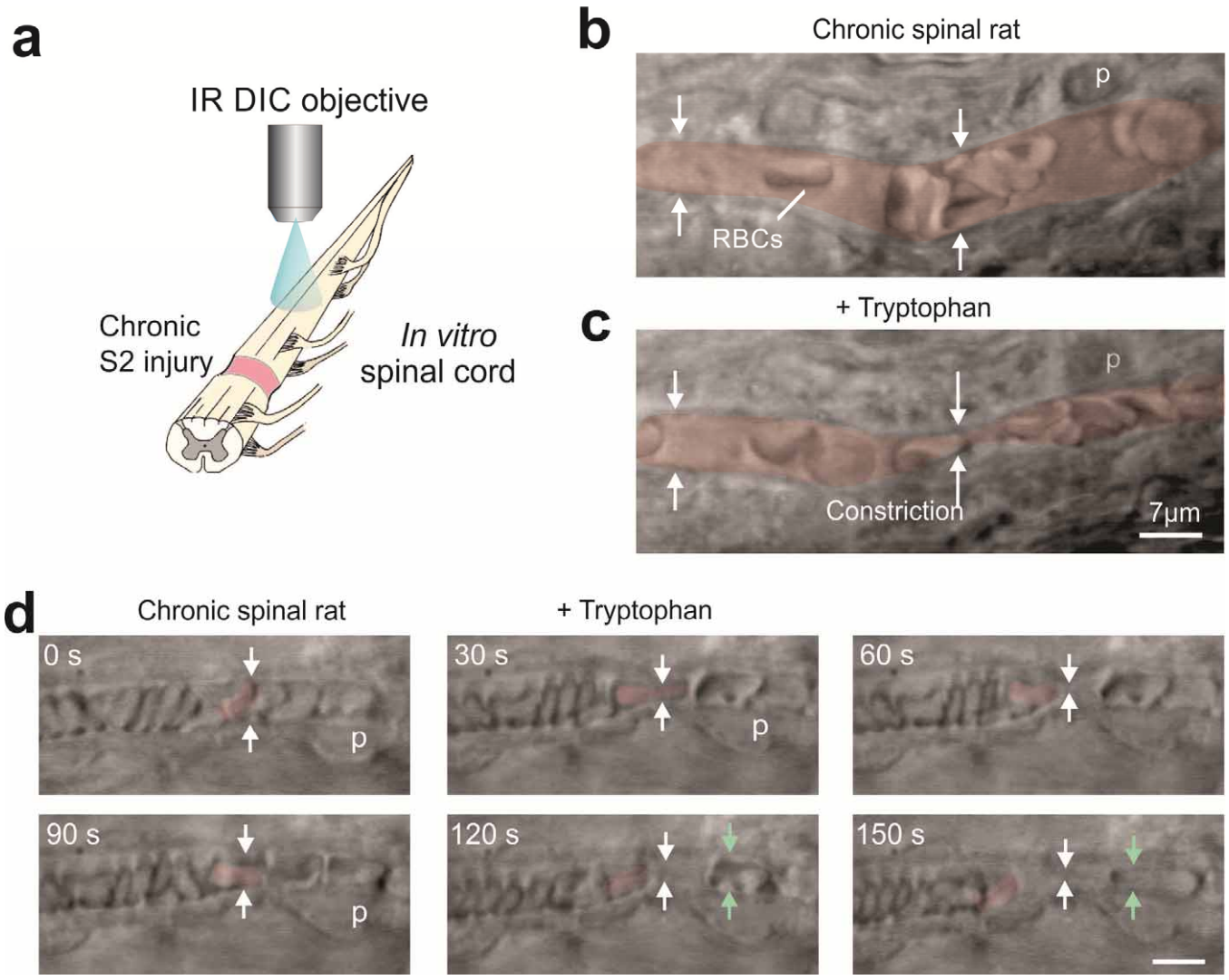

Supplementary Figure 3. Tryptophan and tryptamine induces both tonic and rhythmic contractions of capillaries. **(a)** Schematic of spinal cord preparation for *in situ* imaging of capillaries with IR DIC microscopy in the whole sacral spinal cord from chronic spinal rats, maintained *in vitro*. **(b)** Image of a spinal capillary in the cord caudal to a chronic sacral transection (3 months post injury), with red blood cells (RBC) and lumen pseudo-colored red for clarity, and pericyte nucleus labelled p (edge of pericyte extends to top right arrow). **(c)** Application of tryptophan (30 µM) *tonically* constricted this capillary adjacent to the pericyte (right arrows; starting at 1 mins post application; usually within 10 µm of the outer edge of the soma); but not at locations without nearby pericytes (left arrows). Such tonic constrictions occur in 75% of capillaries (of $n = 84$). **(d)** In other capillaries (25%), tryptophan produces a *rhythmic capillary motion*, with the capillary constricting at about 30 - 60 s after tryptophan application (at white arrows adjacent to pericyte, p), and then partially relaxing at 90 - 120 s, and then further constricting at about 150 s (with additional areas constricting, green arrows). This slow rhythmic contraction repeats throughout tryptophan application (1 hr). During the peak of the constriction it completely obstructs the capillary, displacing RBSs, but then it partial re-opens rhythmically, which would allow a very slow flow rate, below the minimum flow possible with tonic contractions. One RBC is pseudo colored red to show its motion. See *Supplementary Video* for motion of the same capillary (sped up 16x real time). Such rhythmic capillary constrictions have been described previously in the periphery[1], but not in the CNS. Tryptamine (10 - 100 µM) likewise produced rhythmic contractions of capillaries, and also caused rhythmic contractions of arteriole and artery walls, though endogenously produced tryptamine from applied tryptophan had no effect on arterioles/arteries.

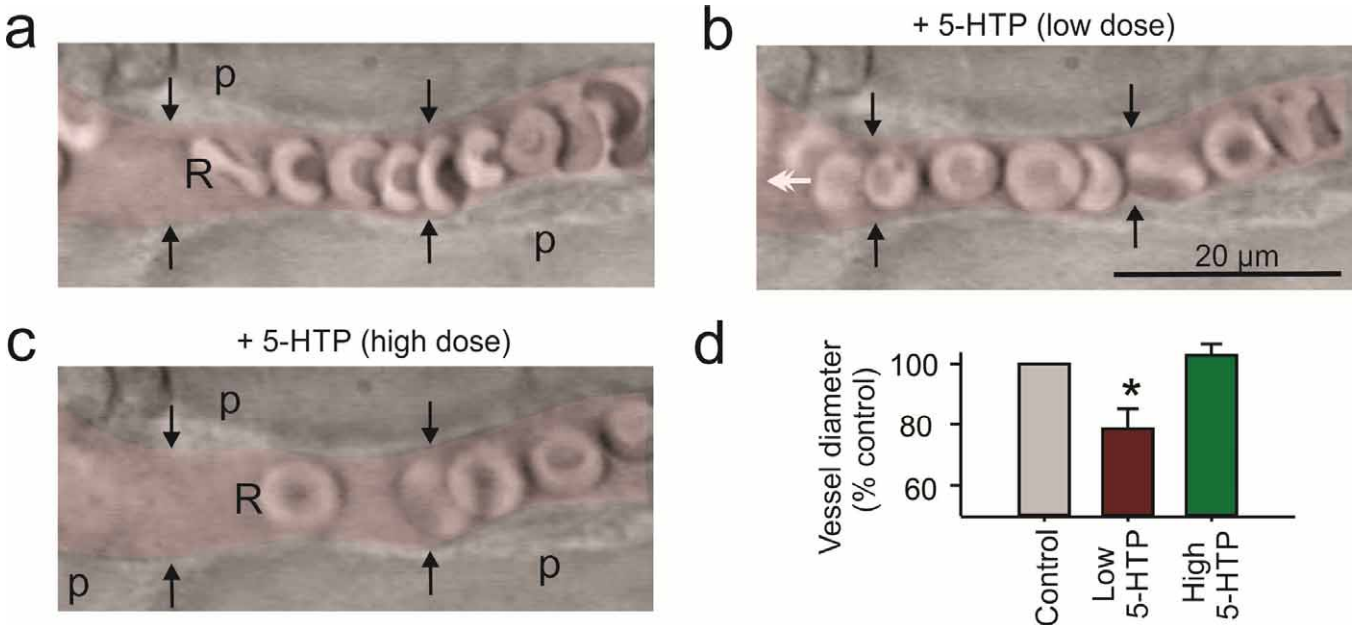

Supplementary Figure 4. Bimodal action of 5-HTP on capillary diameter. **(a)** Image of spinal capillary (DIC image ~200 µm below pia) in the cord caudal to a chronic sacral transection (2 months pot injury). Red blood cells (RBC) and the region within endothelium (thin white band) are pseudo-colored red for clarity. This image was taken in a live whole sacral cord maintained *in vitro*. **(b)** Application of 5-HT precursor 5-HTP at a low dose (0.1 µM) constricted the capillary adjacent to pericytes, and displaced RBCs to the left (white arrow; at 3 mins post dose). **(c)** Application of a subsequent higher dose of 5-HTP (1 - 10 µM) induced the opposite action, dilating the capillary. This dilation was mimicked by the 5-$HT_{2B/C}$ receptor agonist alpha-methyl-5-HT (0.3 µM, 37.1 ± 4.2% diameter increase, $n = 5$). **(d)** Group means of vessel diameter measurements with 5-HTP ($n = 23$ low dose, $n = 10$ high dose), compared to pre-drug control (100%), in the sacral cord caudal to a chronic transection SCI. *$P<0.05$, relative to pre-treatment. Error bars, s.e.m. Notice again that only a low dose 5-HTP constricts vessels, and higher doses cause a dilation that returns the vessels to control levels. We suggest that this is due to the activation of 5-HT_2 receptors that dilate the vessel at higher doses of 5-HTP. We do not know where these receptors are located, but we do know that 5-HT_2 receptors increase neuronal activity (Murray et al. 2010), and thus dilation might occur via neurovascular coupling. Regardless, there appears to be a balance of constriction and dilation mediated by 5-HT_{1B} and 5-HT_2 receptors, respectively. The reduction of the action of tryptamine and tryptophan with increasing dose is also explained by these two receptors, with 5-HT_{1B} receptors first constricting vessels via low tryptamine doses, and then 5-HT_2 receptors likely reducing the constriction at higher doses.

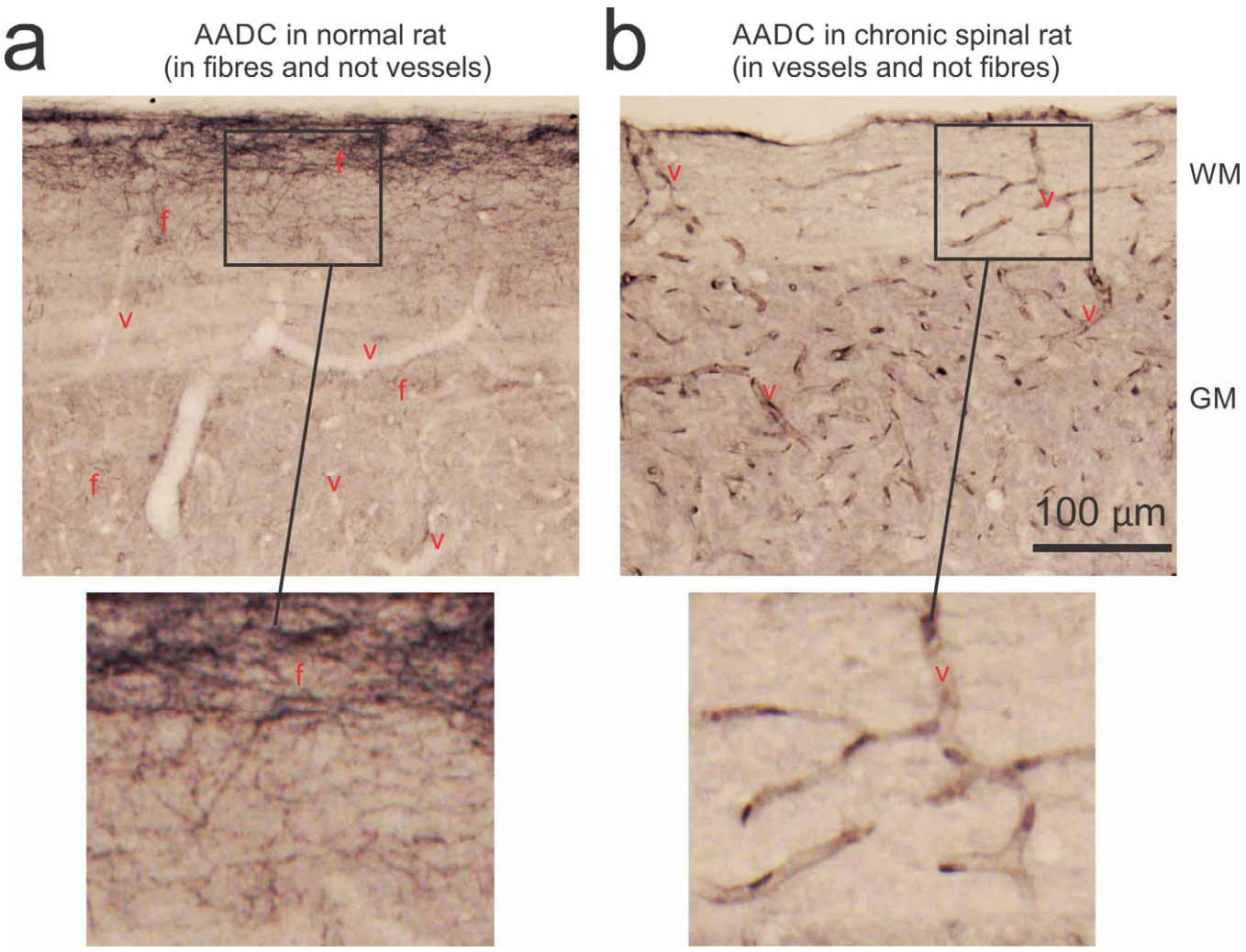

Supplementary Figure 5. In uninjured rats AADC is expressed mostly on descending monoamine axons (fibres, f), but after SCI these fibres are lost and then AADC is instead expressed mostly on vessels (v, capillaries). **(a)** Immunolabelling for AADC in a normal rat (DAB stain, brown), shown in a horizontal sacral spinal cord section, with descending brainstem-derived monoamine fibre bundles in the white matter (WM) and collaterals projecting diffusely into the grey matter (GM). **(b)** AADC expression on fibres is lost completely in a chronic spinal rat (sacral S2 transection, 2 months post injury) below the injury, because these brainstem-derived fibres are eliminated with injury. Instead AADC is highly upregulated on vessels, especially in pericytes on capillaries (dark patches on vessels)[2]. Section shows dorsal horn white matter (WM) and gray matter containing vessels with AADC. AADC is expressed on all capillaries in both the white and gray matter. The white matter normally contains fewer capillaries, and these run lengthwise (rostro-caudally), so less AADC labelled vessels are seen in the white matter, and these are best visualized in sagittal sections (as here), rather than transverse section (Fig 2a).

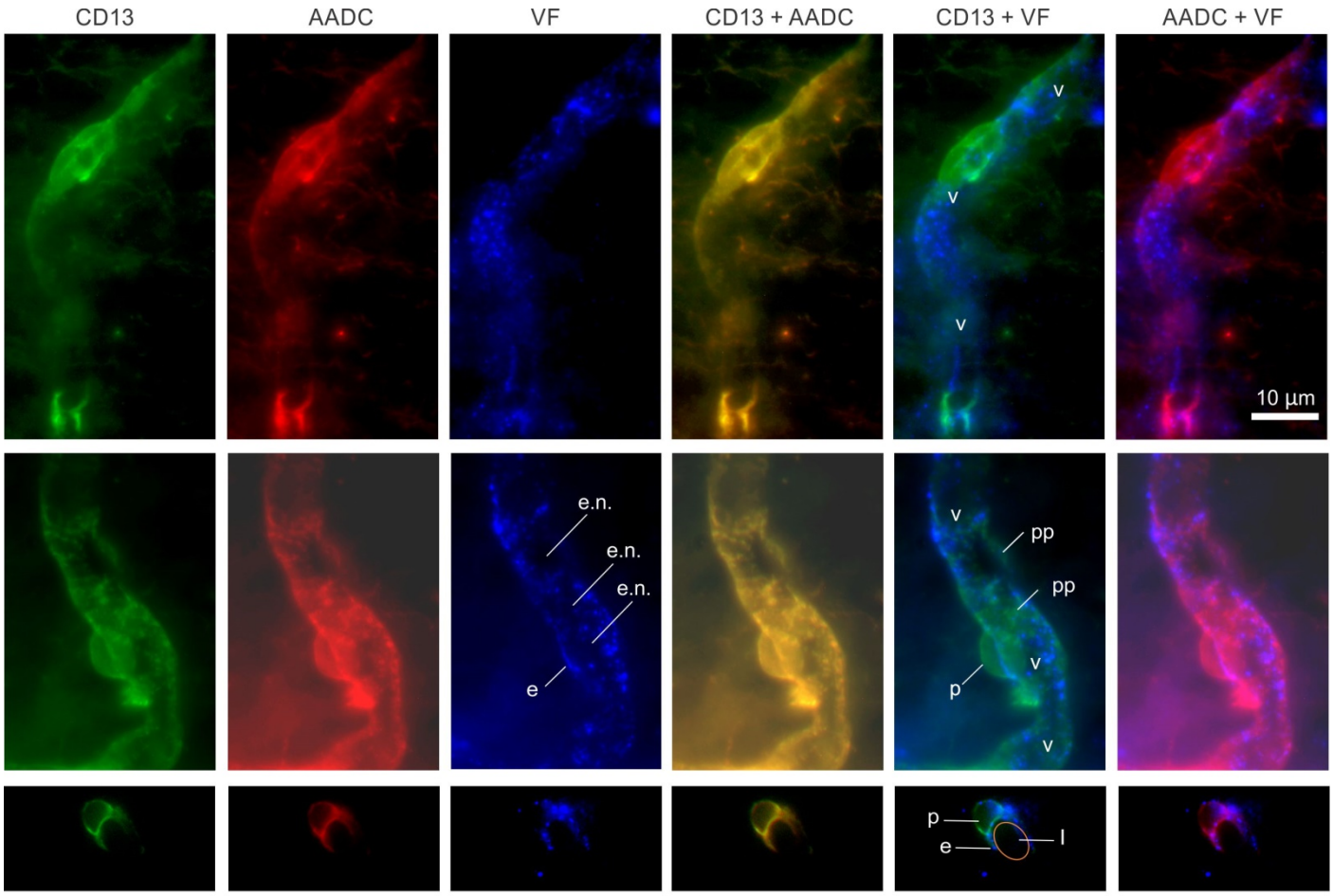

Supplementary Figure 6. AADC is co-localized with pericytes and not endothelial cells on capillaries after SCI. Capillaries (v) from chronic spinal rat, in sacral cord below transection (2 month post injury). The endothelium (e) is labelled with Von Willebrand Factor (VF), which labels storage granules (blue dots) in endothelium. The large gaps (black) in labelling are where the disc-like endothelial nuclei (e.n.) displace the granules[3]. The pericytes are labelled with CD13[4] (green), which labels cell bodies (p) as well as extensive fine processes (pp). Importantly, CD13 (aminopeptidase; APN) has previously been shown to be absent from endothelial cells, and highly expressed in pericytes[4]. Lower panels shows a cross section through a vessel and pericyte, with vessel lumen (l) labelled with orange circle. AADC (red) again co-localizes extensively with pericytes (CD13+AADC, yellow), but not the endothelium (VF).

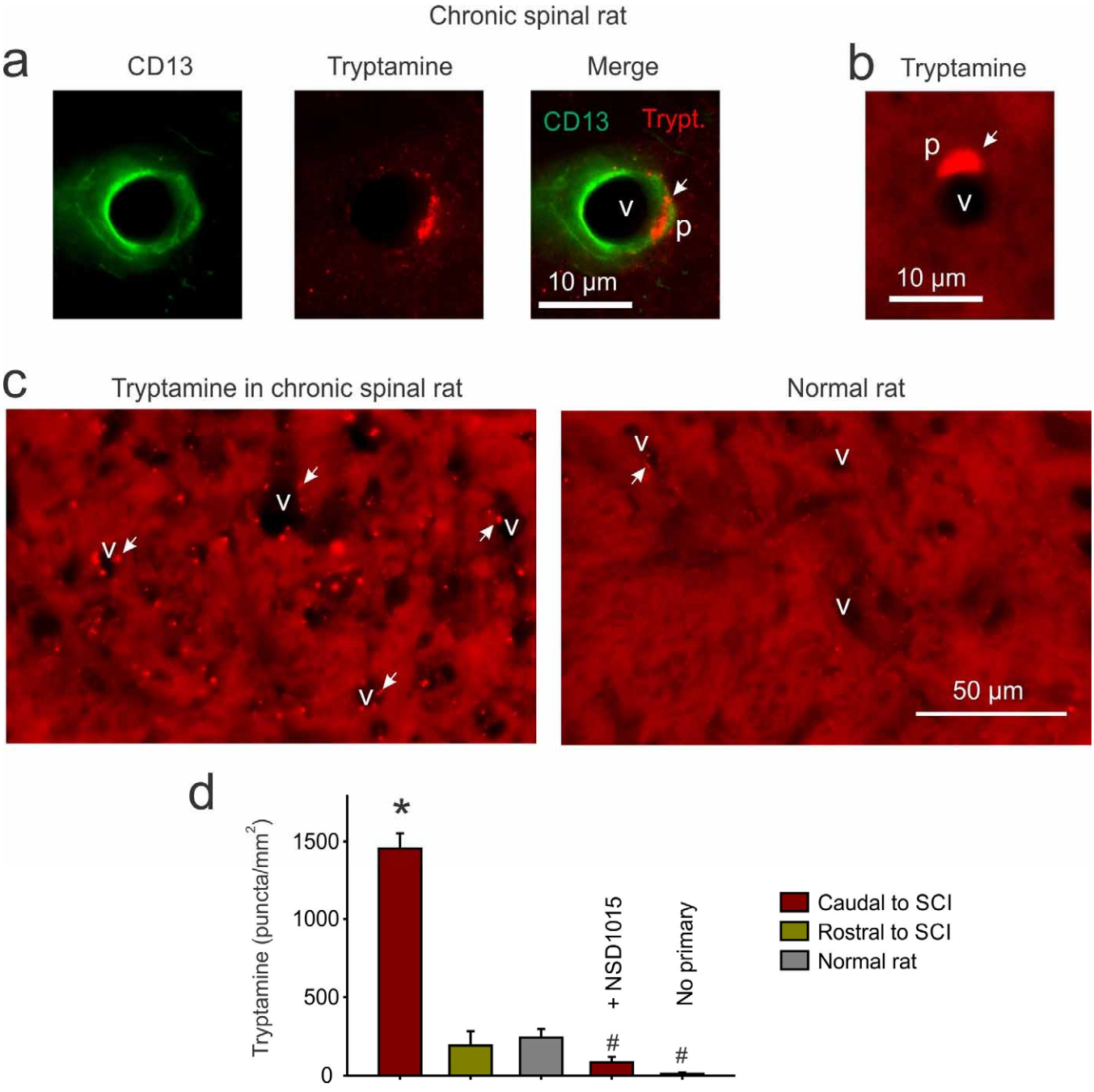

Supplementary Figure 7. Endogenous tryptamine production in pericytes after SCI, and relative lack of tryptamine in uninjured rats. **(a-b)** Caudal to a sacral spinal cord transection (2 months post injury) immunolabelling shows tryptamine (red) densely accumulated in the soma of pericytes (p) on capillaries (v). Pericyte labelled with CD13 (green). Tryptamine labelling is generally in the form of dense punctate granules, which accumulate into larger clusters in the soma. **(c)** Lower magnification images of tryptamine immunolabelling in spinal cords from injured and uninjured rats, with images brightened to show the structure of tissue and in particular blood vessels (black areas, v). CD13 immunolabelling did not always work well with the glutaraldehyde needed for tryptamine immunolabelling, and so we used these brightened images to quantify tryptamine, without CD13. Punctate granules (arrows) with intense tryptamine immunolabelling were considered positive for tryptamine, and appeared on most capillaries

(v) after SCI, whereas in normal uninjured rats most vessels lacked these tryptamine granules (examples labelled v without arrow). **(d)** Tryptamine was quantified by counting the number of punctate granules per unit area. Tryptamine quantity was significantly higher caudal to the SCI, compared to normal, and this tryptamine labelling was eliminated by pretreating rats with NSD1015 (3 mM, topically applied 30 min prior to perfusion in chronic spinal rats), or by removing the primary antibody in the labelling procedure. *$P < 0.05$, significantly larger than normal; # significantly smaller than normal or SCI expression. Error bars, s.e.m.

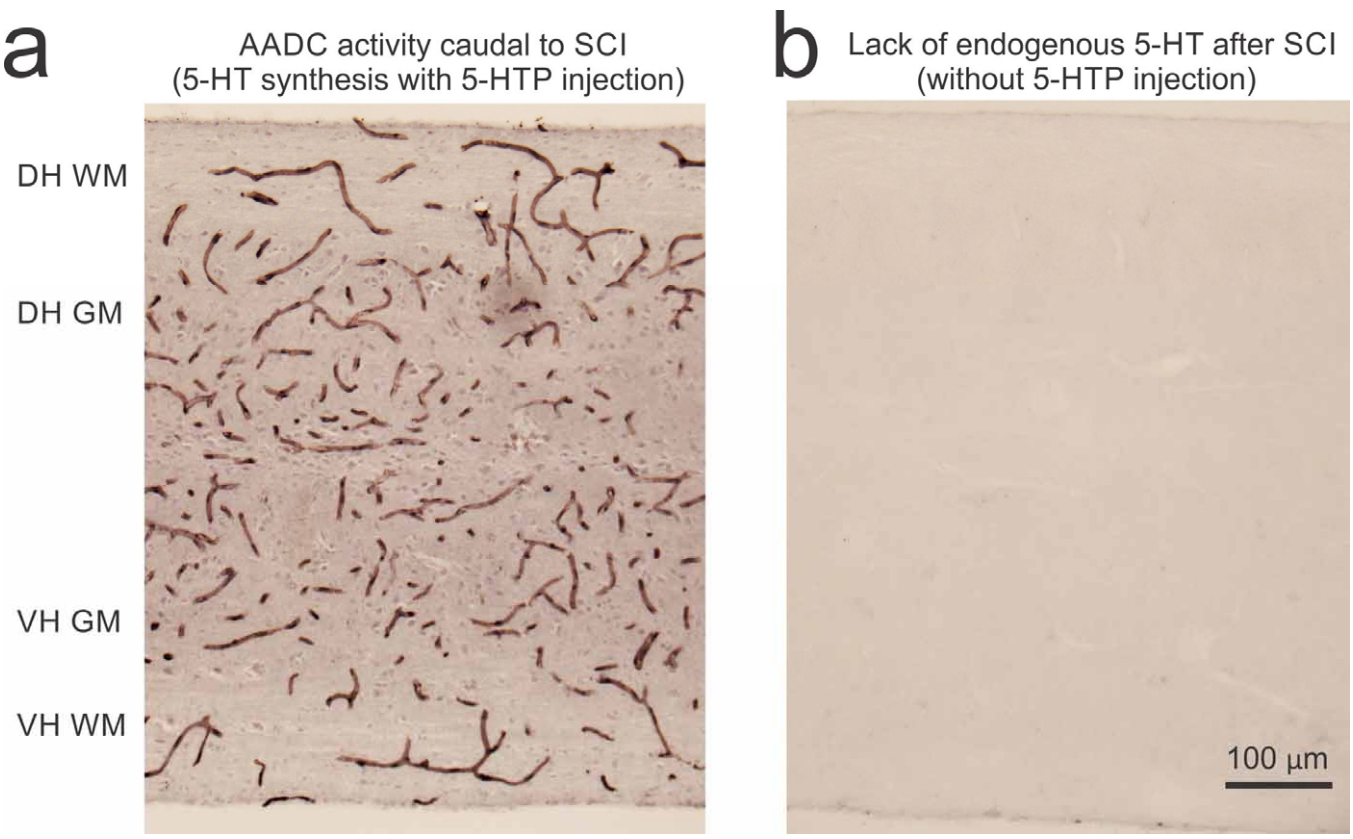

Supplementary Figure 8. AADC is highly active in capillaries throughout the spinal cord of chronic spinal rats. **(a)** Immunolabelling for 5-HT in a 5-HTP-treated chronic spinal rat, shown in a sagittal section caudal to the transection (DAB, dark labelling; rat treated 25 mins prior to perfusion with 30 mg/kg 5-HTP i.p.). AADC produces 5-HT from applied 5-HTP, and thus 5-HT immunolabelling acts as a surrogate marker for AADC's ability to produce amines after SCI (AADC equally well produces tryptamine and 5-HT [5-hydroxytryptamine], these two only differing by an OH^- group). AADC activity (5-HT) is seen in capillaries throughout the cord caudal to the SCI, in the dorsal horn (DH) and ventral horn (VH), both in the white matter (WM) and gray matter (GM). Note that most white matter vessels run horizontally, and are more readily seen in these long sagittal sections, rather than transverse sections (Fig 2). **(b)** Immunolabelling for 5-HT in a similar section of spinal cord in another chronic spinal rat, but without 5-HTP treatment. In these untreated chronic spinal rats, the spinal cord completely lacks endogenous 5-HT caudal to the injury.

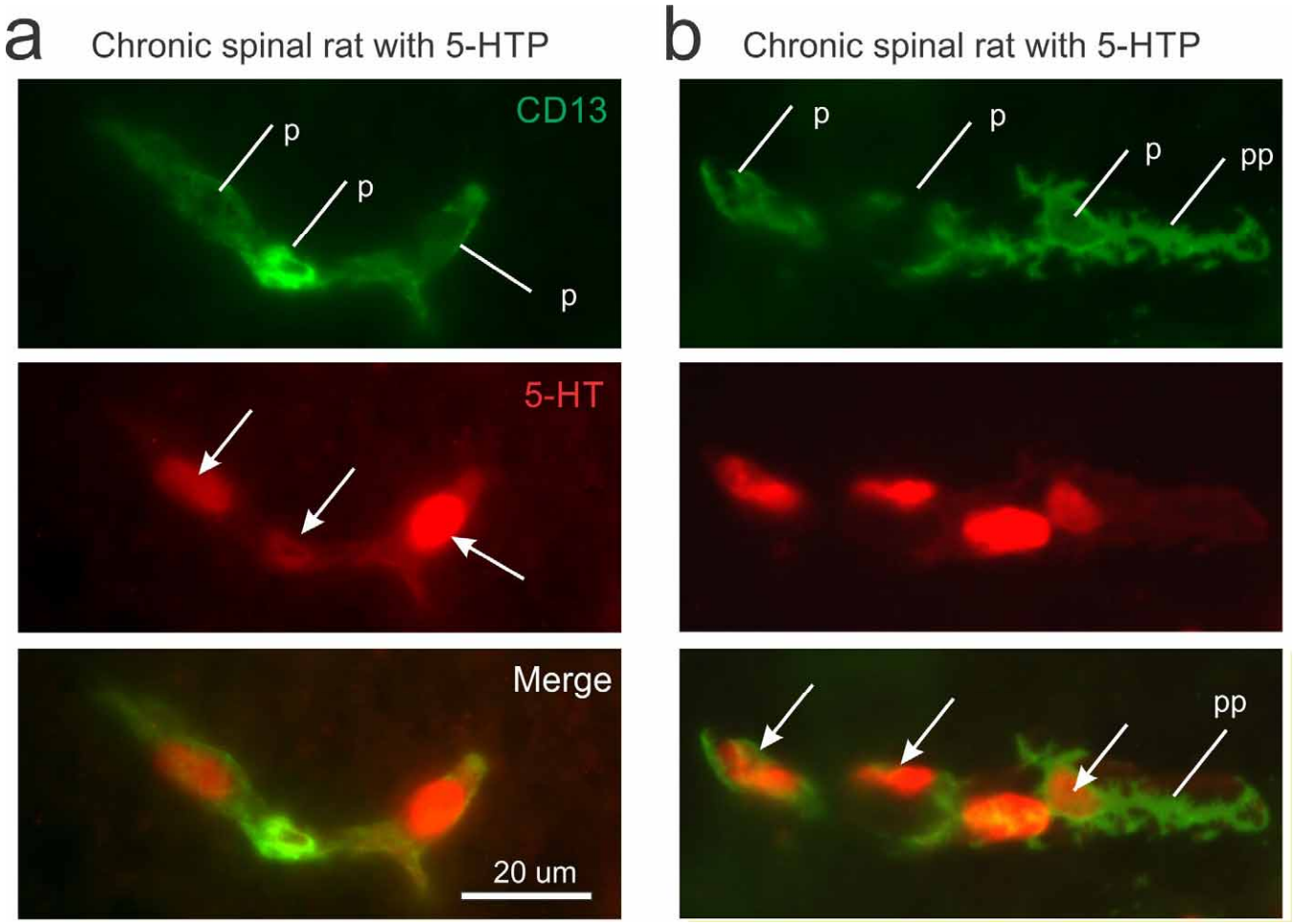

Supplementary Figure 9. Products of AADC are accumulated in the soma of pericytes after SCI. **(a -b)** Two representative examples of pericytes on capillaries of chronic spinal rat caudal to the transection (2 month post injury), labelled with CD13. CD13 labels the soma (p) as well as the fine pericyte processes (pp). The rat was injected with 5-hydroxytryptophan (5-HTP) prior to fixation, which is decarboxylated by AADC in the pericyte to produce 5-hydroxytryptamine (5-HT; no 5-HT occurs without an injection; see Supplementary Fig 8). Immunolabelling for 5-HT (red) shows that this AADC product (5-HT) is accumulated at the pericyte soma (p; at arrows), but not in the pericyte processes (pp). Note that CD13 labels the pericyte soma less intensely than NG2 in Fig 2, but it labels the rest of the pericyte thoroughly, and so we used CD13 here. CD13 labels the pericyte membrane, whereas 5-HT is in the cytoplasm, and thus appears ringed by CD13.

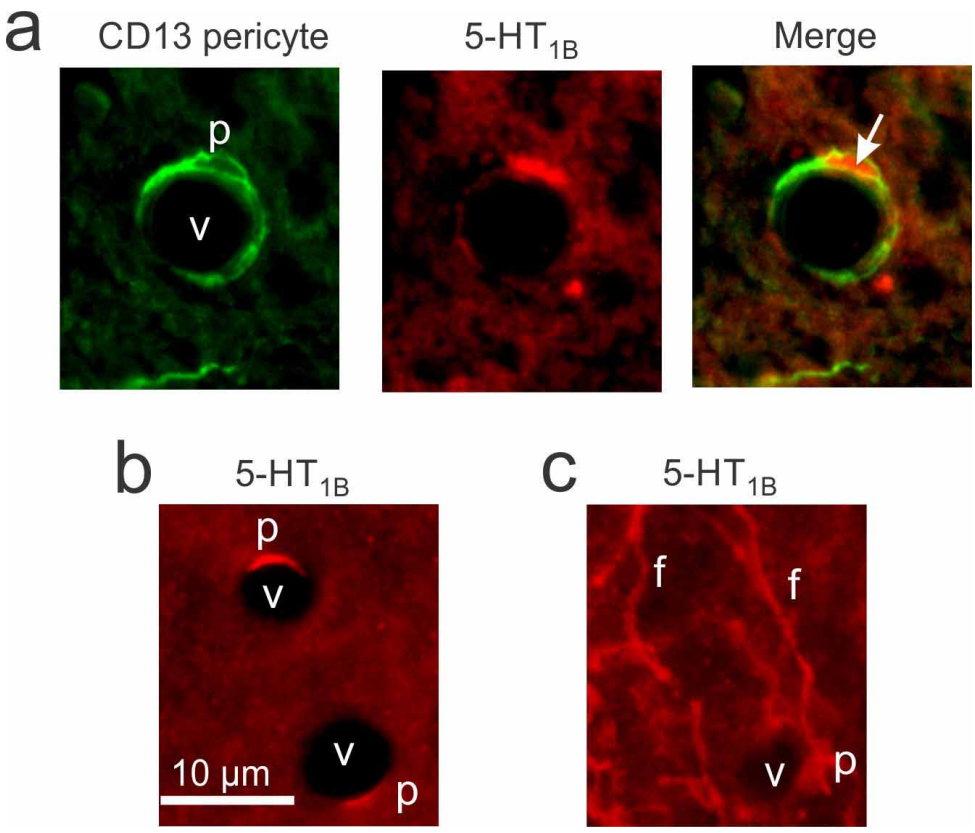

Supplementary Figure 10. 5-HT_{1B} receptors on pericytes and dorsal root axons. **(a)** Immunolabelling for 5-HT_{1B} receptors (red), with strong expression on a CD13-labelled pericyte (p, green) on a capillary (v) in the spinal cord caudal to a SCI (sacral, 2 months post injury), consistent with other studies of 5-HT receptor expression in normal animals[5]. Arrow points to 5-HT_{1B} receptor labelling in the cytoplasm of the pericyte soma. **(b)** Additional examples of 5-HT_{1B} immunolabelling on capillary pericytes. **(c)** Outside of vessels, immunolabelling of 5-HT_{1B} receptors was also observed on fine axon fibers (f) in the superficial dorsal horn, some of which clearly entered the dorsal root (likely unmyelinated sensory afferents). These fine fibres were confined to the dorsal entry zone, whereas the effects of 5-HT_{1D} ligands (GR127935 and zolmitriptan) on vessels occurred throughout the cord caudal to the SCI (Fig 1). n = 5 tested with similar results.

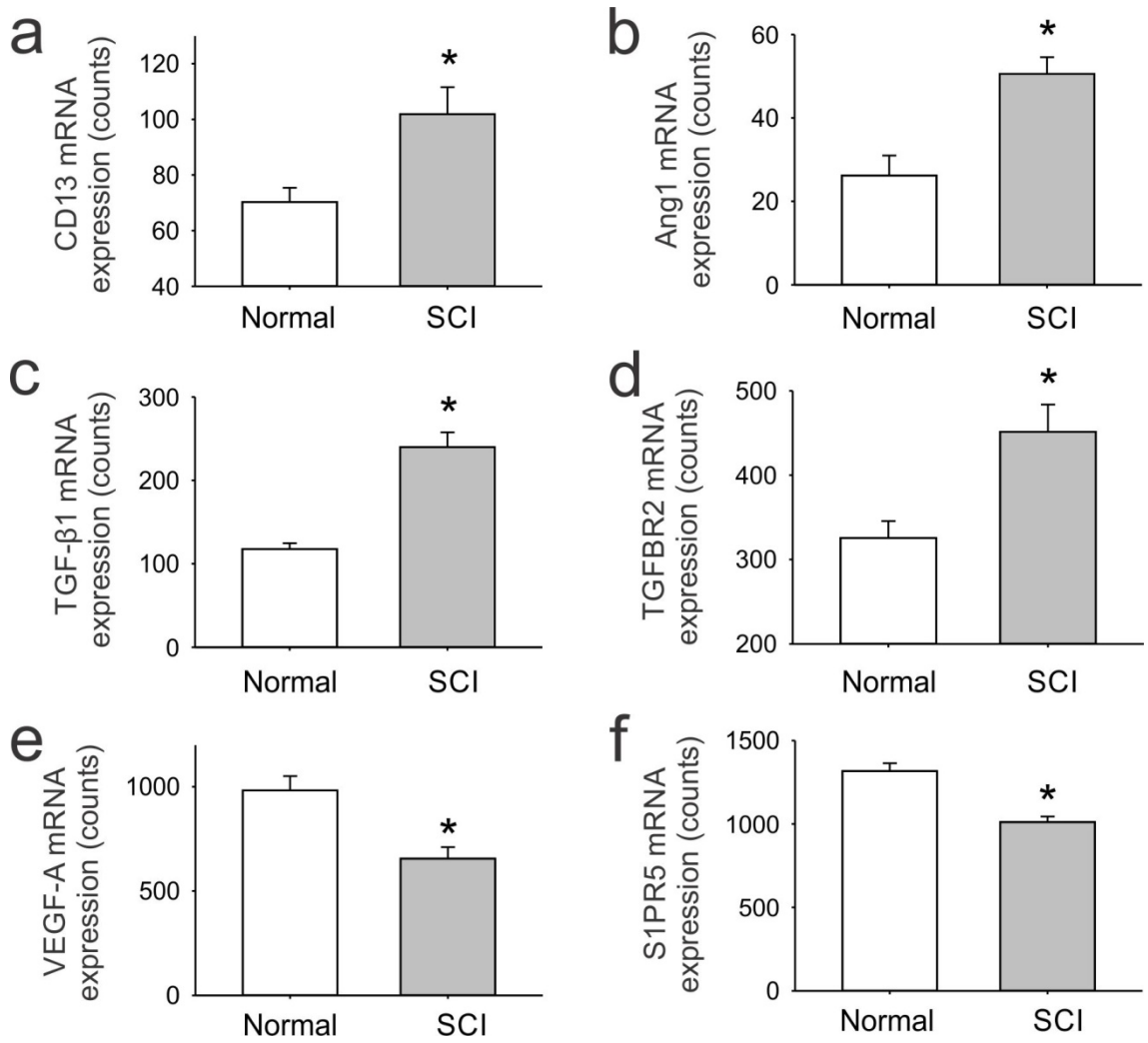

Supplementary Figure 11. Changes in expression of mRNA for pericyte-related signalling molecules after SCI. **(a)** Expression of mRNA for the selective pericyte marker CD13 (encoded by *Anpep* gene)[4] was increased with SCI, compared to in normal rats. Expression was measured with RNA-seq analysis as we described previously[6], using tissue from the whole spinal cord caudal to the sacral S2 lesion level, *not* including lesion site. **(b-d)** Expression of mRNA for many pericyte-related signalling molecules was also increased with SCI, including: Angiopoietin 1 (Ang1; encoded *ANGPT1*), TGF-β1 (transforming growth factor beta; *TGFB1*) and TGF-β receptor type 2 (*TGFBR2*). Angiopoietin 1 is essential for signalling between pericytes and endothelial cells, leading to maturation and stabilizing of the endothelial cell.[7] TGF-β1 and its receptors transform pericytes, inhibiting proliferation and inducing expression of contractile properties (α-SMA).[7,8] Thus, these changes are consistent with increased mature contractile pericytes after SCI, though this needs further study. **(e-f)** Expression of mRNA for other pericyte-related signalling molecules was decreased with SCI, including VEGF-A (vascular endothelial growth factor; encoded *VEGFA*) and S1PR5 (Sphingosine-1-phosphate receptor; *S1PR5*). VEGF promotes angiogenesis[9] and S1PR5 facilitates the blood-brain barrier, regulated by pericytes and endothelial cells.[10] Expression of mRNA for hypoxia-inducible transcription factor 1 alpha (HIF1a) was unchanged in chronic SCI compared to normal rats (not shown), suggesting that previously described early HIF1a response to acute SCI[11] is blunted over time (two months after SCI). Also, expression of mRNA for 5-HT_{1B} receptors (htr1b) was unchanged with SCI (not shown). All plots show means (and s.e.m.) of mRNA counts for each gene that were adjusted to total library counts in each rat (normalized RNA-seq counts).[12,13] n = 8 normal rats (age matched) and n = 8 chronic spinal rats (8 weeks post injury); *Nominal $P < 0.05$: significant difference with SCI compared to control normal rats.

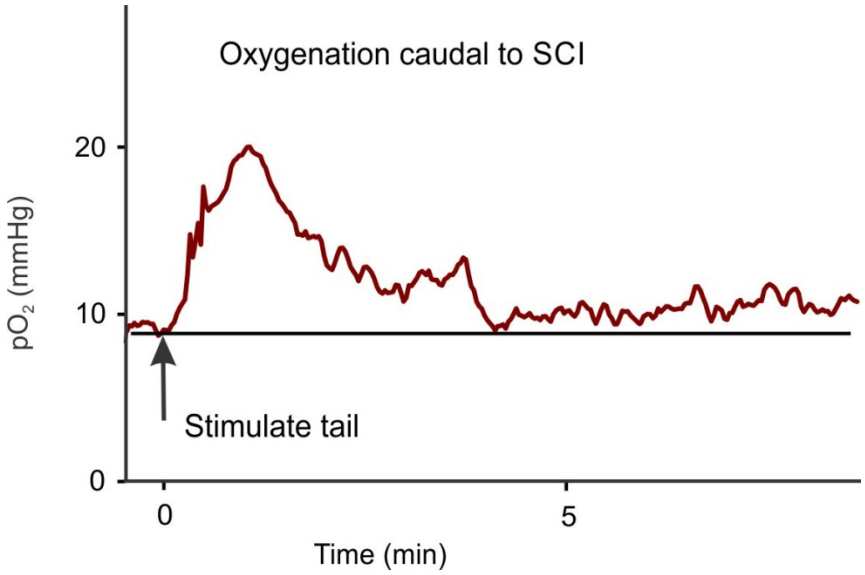

Supplementary Figure 12. Neurovascular coupling caudal to a SCI. Brief mechanical stimulation of the tail (1 sec light rub along tail, at arrow) that provides sensory input to the sacral spinal cord produces a prolonged increase in oxygenation of the sacral cord caudal to a transection in chronic spinal rats (S2 transection, 2 months post injury). Oxygen (pO_2) measured with an optical sensor (optode) in the dorsal horn of the S4 sacral spinal cord, as in Fig 3. This prolonged increase in oxygen reflects classical neurovascular coupling, whereby neuronal activity dilates vessels and increases oxygenation[14]. The pronounced neurovascular coupling seen here in chronic spinal rats likely helps explain the prolonged increase in motor activity (EMG) observed after a brief inhalation of enhanced oxygen (Fig 4e). That is, during a brief inhalation of high oxygen, the spinal cord pO_2 increases (Fig 3e), which in turn increases neuronal activity (Fig 4), which then leads to neurovascular coupling which dilates vessels and increases the neuronal activity further (Fig 4e). This process is repeated with neurovascular coupling, further increasing oxygenation, and so on, leading to prolonged motor activity. Likely, this prolonged motor activity is exaggerated after injury because neurons are hyperexcitable[15], and only terminates after 20 mins, similar to how EMG reflexes diminish over time, habituating slowly to repeated stimulation.

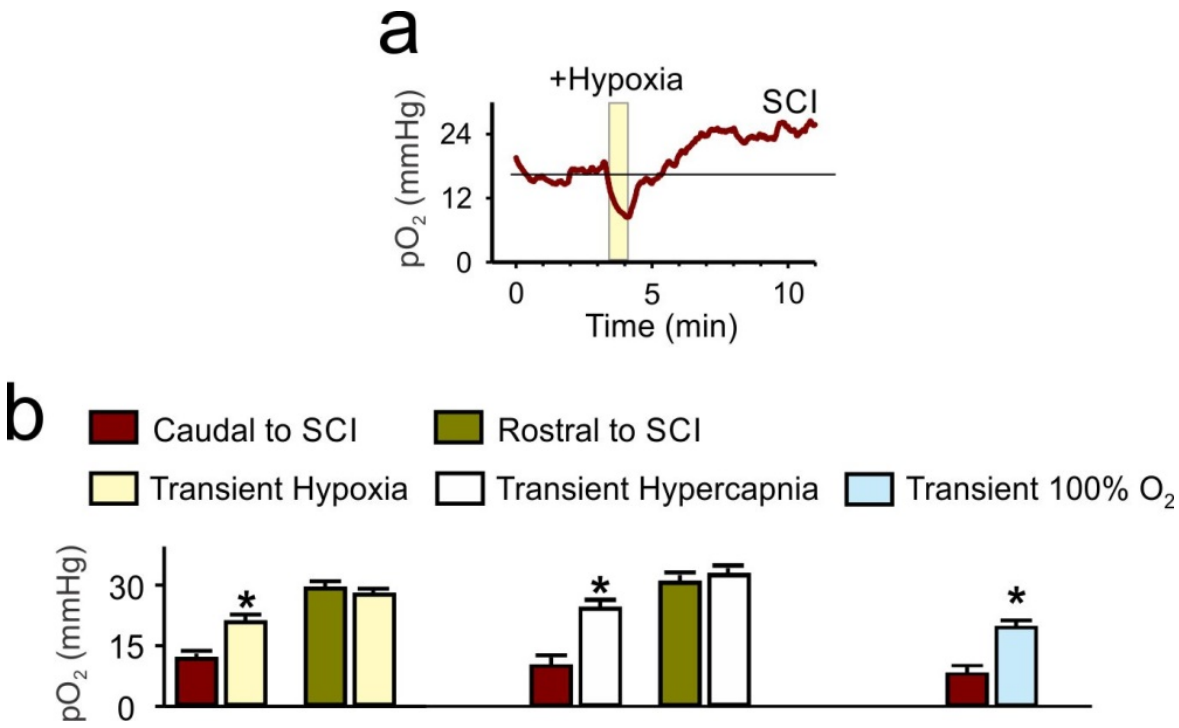

Supplementary Figure 13. Hypoxic, hypercapnic or hyperoxic breathing is followed by a rebound increased oxygenation in the spinal cord of rats with SCI. **(a)** Partial pressure of oxygen (pO_2) measured in the spinal cord with an optical sensor (optode), caudal to the SCI in chronic spinal rats (S2 transection, 4 months post injury). Under baseline conditions the cord was hypoxic. A brief episode of hypoxic breathing (1 min breathing 10.5% O_2, rather than usual 21% O_2 in air) induced an immediate decrease in pO_2 (at yellow bar) further increasing the cord hypoxia. However, this was followed by a sustained increase in pO_2 that lasted 15 - 20 min, while elsewhere pO_2 returned rapidly to normal (within 1 - 2 min rostral cord pO_2 and arterial pO_2 returned to normal; see Methods). **(b)** Group means of pO_2 prior (red, green) and 15 mins after transient hypoxia (n = 7), hypercapnia (30 s breathing air with 10% CO_2, n = 5), or hyperoxia (1 min 100% O_2, n = 7) breathing, with all treatments increasing pO_2 caudal to the SCI. Rostral measurements (green) not tested with hyperoxia. *$P < 0.05$: significant difference relative to pre-treatment conditions. Error bars, s.e.m. To examine permanent hypoxia we cut the sacral spinal cord blood supply to remove all oxygen supply (transecting the cord acutely). This led to a rapid drop in pO_2 to zero (within 2-5 seconds; whereas the pO_2 of saline on the exposed cord surface remained near that of air: > 150 mmHg; not shown), demonstrating that the cord avidly consumes oxygen and the low pO_2 caudal to the SCI reflects inadequate blood flow to meet oxygen consumption (ischemic hypoxia).

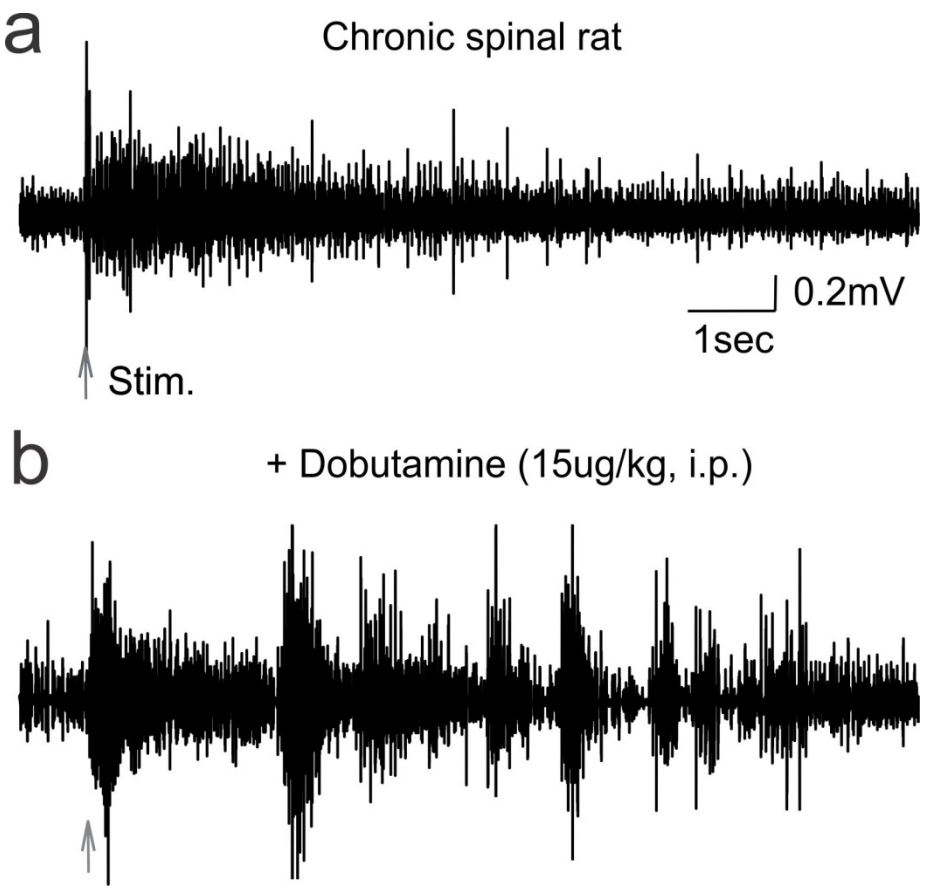

Supplementary Figure 14. Peripherally increasing blood pressure to indirectly increase spinal cord blood flow increases motor activity. **(a)** EMG recording from tail muscles of a chronic sacral spinal rat (2 months post injury) with electrical stimulation of the tip of the tail to evoke long lasting motor activity (at arrow, stim. 50×T, reflex threshold). **(b)** Systemic application of a very low dose of the β-adrenergic receptor agonist dobutamine (15 µg/kg. i.p.) increased the overall EMG activity, and additionally revealed rhythmic burst of EMG, similar to the action of inhaled O_2 in Fig 4d. Similar increased EMG was observed in 5/5 rats tested (peak effect measured 2 - 3 mins post dobutamine). This very low dose dobutamine is known to increase heart output and blood pressure[16], and indeed dobutamine is a common sympathomimetic drug used clinically to treat heart failure. The increased blood pressure with dobutamine indirectly increases blood flow in the spinal cord, and thus these experiments establish a link between increased spinal cord blood flow and improved motor function. Increasing blood pressure with vasopressin produced a similar increase in EMG (not shown). Higher doses of dobutamine (100 - 300 µg/kg) are known to instead decrease blood pressure, via a peripheral vasodilation, secondary to the primary effect on heart output[16]. Accordingly, we observed that 100 µg/kg dobutamine decreased EMG in these same rats (not shown), consistent with decreased spinal cord blood flow from lower blood pressure. Dobutamine had no effect on the isolated cord from chronic spinal rats (in vitro, see Supplementary Fig 16 for details of *in vitro* method) at concentrations equivalent to the doses used *in vivo* (1 - 50 nM, not shown). Thus, the action of dobutamine was primarily in the periphery to modulate blood pressure.

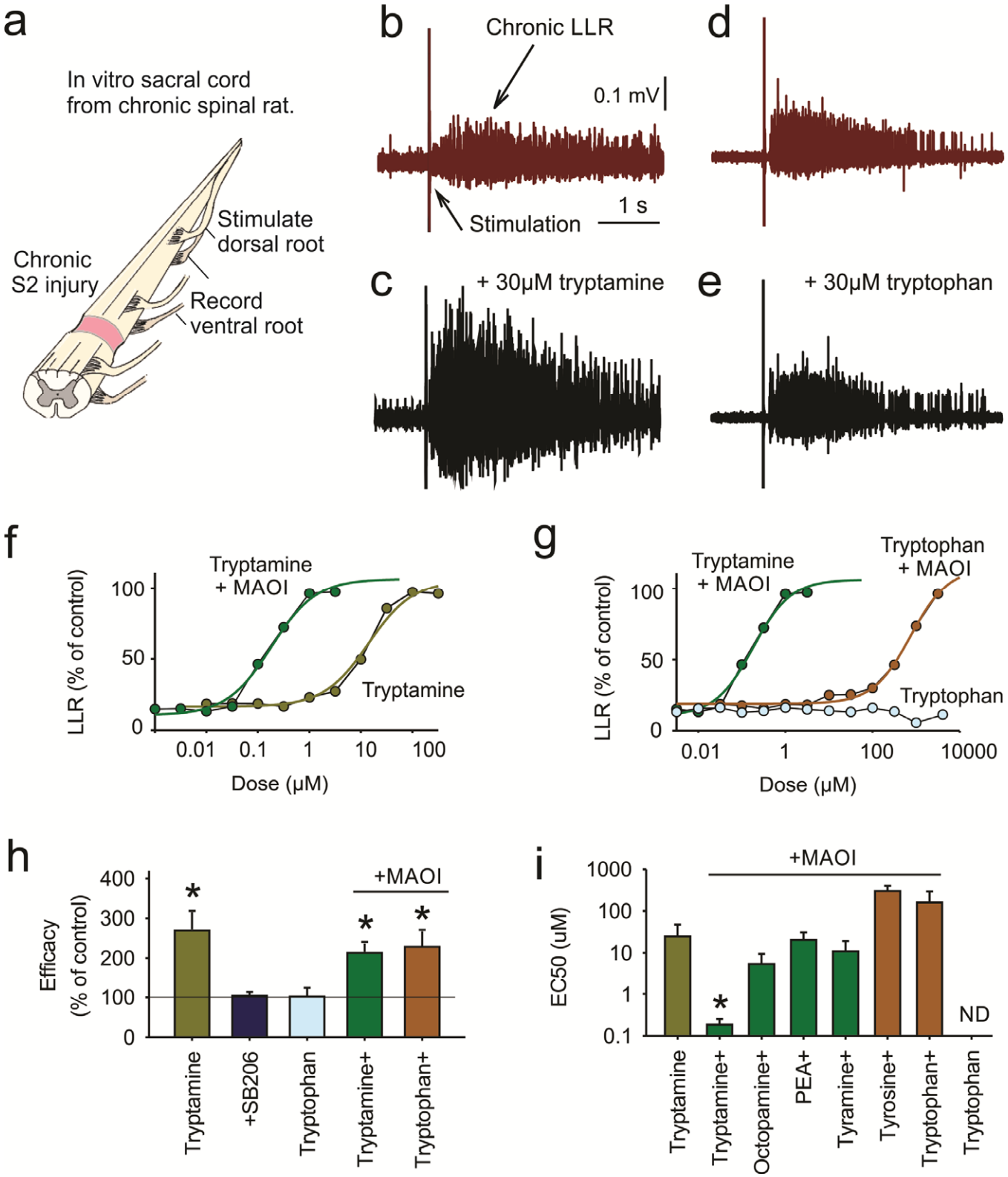
a
In vitro sacral cord
from chronic spinal rat.
Stimulate
dorsal root
Chronic
S2 injury
Record
ventral root
b
Chronic LLR
0.1 mV
1 s
Stimulation
d
c
+ 30μM tryptamine
e
+ 30μM tryptophan
f
Tryptamine
+ MAOI
Tryptamine
LLR (% of control)
100
50
0
0.01
0.1
1
10
100
Dose (μM)
g
Tryptamine
+ MAOI
Tryptophan
+ MAOI
Tryptophan
LLR (% of control)
100
50
0
0.01
1
100
10000
Dose (μM)
h
+MAOI
Efficacy
(% of control)
400
300
200
100
0
*
*
*
Tryptamine
+SB206
Tryptophan
Tryptamine+
Tryptophan+
i
+MAOI
EC50 (uM)
1000
100
10
1
0.1
*
ND
Tryptamine
Tryptamine+
Octopamine+
PEA+
Tyramine+
Tyrosine+
Tryptophan+
Tryptophan

Supplementary Figure 15. Endogenously produced trace amines do not directly affect motoneuron activity after SCI, even though exogenously applied trace amines do. **(a)** Schematic of the isolated sacral spinal cord from chronic spinal rat, maintained *in vitro*, with roots mounted for stimulation and recording of motoneuron activity and reflexes. **(b)** Long lasting reflex (LLR) recorded from ventral root in response to dorsal root stimulation pulse (0.1 ms, 3xT). **(c)** Increased LLR in response to exogenous application of the trace amine tryptamine. **(d-e)** In contrast, motoneuron activity (LLR and spontaneous activity prior to stimulation) was *not* increased by tryptophan application, indicating that tryptamine endogenously produced by spinal sources of AADC (in vessels; Fig 2) does not influence neurons. **(f-g)** Dose-response relations for LLR (amplitude) with increasing dose of tryptamine and tryptophan. Inhibiting MAO (MAOI) with clorgyline and pargyline (2 μM each) increased the potency of tryptamine by 2 orders of magnitude (reducing doses needed to affect the LLR from 10 μM to 0.1 μM), suggesting that MAO normally metabolises most of the tryptamine in the spinal cord. In particular, even if physiological levels of tryptophan (30 μM) produced similar tryptamine levels (via AADC), these would be reduced by 2 orders of magnitude by MAO (to 0.3 μM), far too low to affect monoamine receptors (5-HT_{2C}, see below). Indeed, the same MAOI treatment enabled tryptophan to increase the LLR, but only at very high unphysiological doses (>> 100μM), indicating that tryptamine endogenously produced by AADC from tryptophan is largely metabolized by MAO before it can influence motoneurons (see Discussion in Li et al. 2014[2]). **(h)** Group means of efficacy (maximum respond amplitude, as a percent of pre-drug) of tryptamine and tryptophan, with the 5-HT_{2C} receptors antagonist SB206553 blocking the action of tryptamine, and tryptophan only affective with MAOI. **(i)** Group means of potency (EC_{50}, effective concentration for 50% effect) of trace amines (tryptamine, tyramine, PEA and octopamine) and acids (tyrosine and tryptophan), in the presence of MAOI (indicated with +, tryptamine and tryptophan alone without MAOI are shown for comparison). MAOI significantly decreased the EC_{50} of tryptamine.*P<0.05, relative to pre-treatment. n = 10 per condition. Error bars, s.e.m. Note that tryptamine is most potent (lowest EC_{50}), especially compared to PEA, consistent with 5-HT_{2C} receptors mediating the action of tryptamine on motoneurons, rather than TAARs (which are most sensitive to PEA)[17,18]. Also note that tryptophan, tyrosine and associated trace amines only had substantial effects when MAO was blocked, suggesting that MAO metabolizes AADC products (trace amines) before they can directly affect neuronal activity. A similar lack of effect of amino acids and trace amines on motor activity occurred in the in vitro cord of normal rats (not shown). In summary, physiological doses of amino acids (tryptophan) or trace amines (tryptamine) have no direct effect on the motoneuron activity in normal or chronic spinal rats.

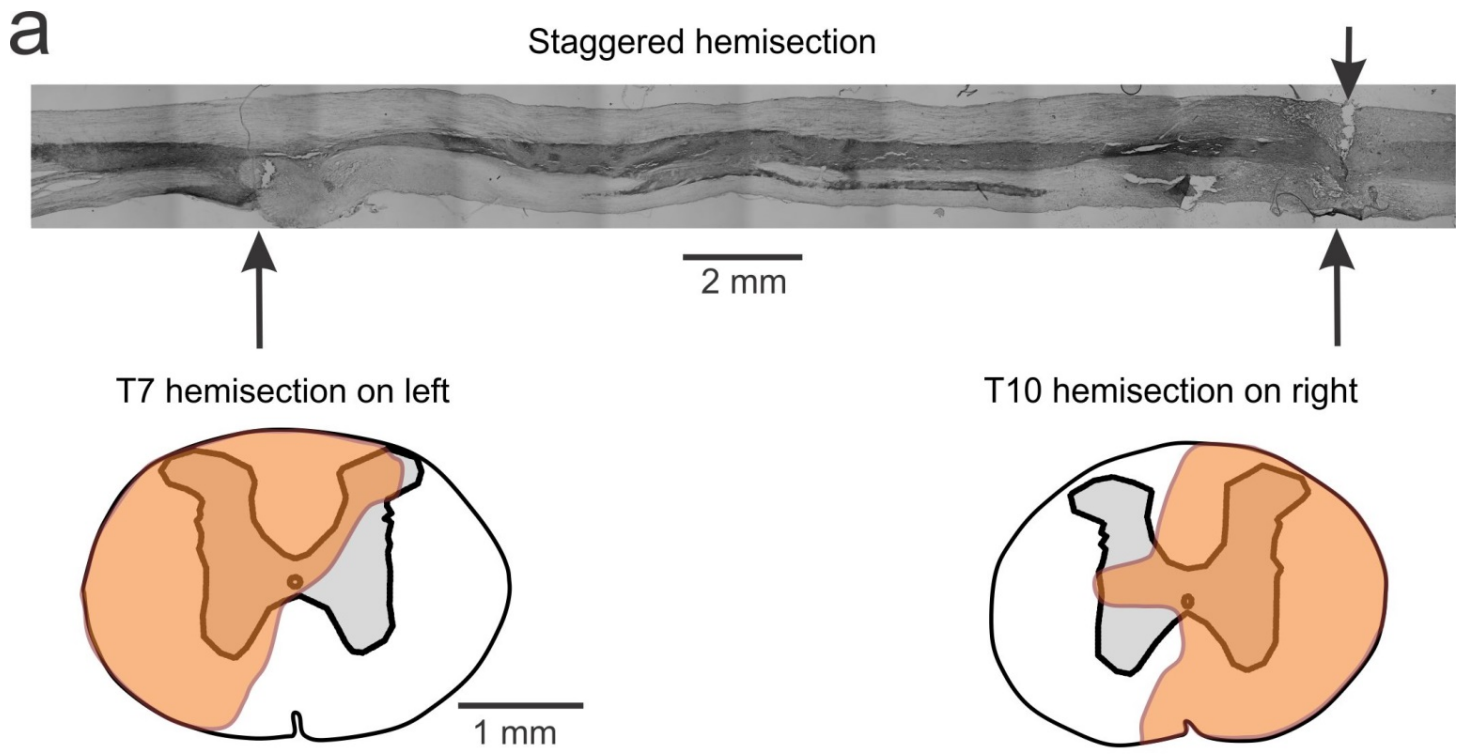
a
Staggered hemisection
2 mm
T7 hemisection on left
T10 hemisection on right
1 mm

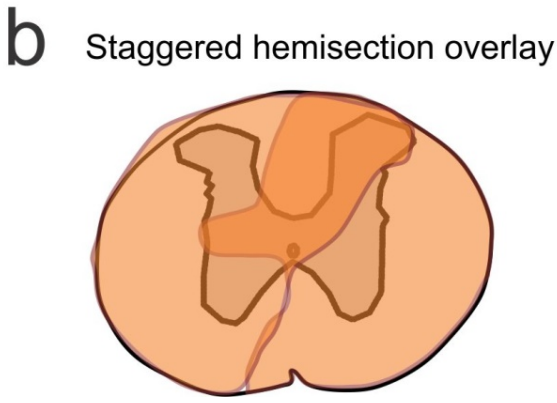
b
Staggered hemisection overlay

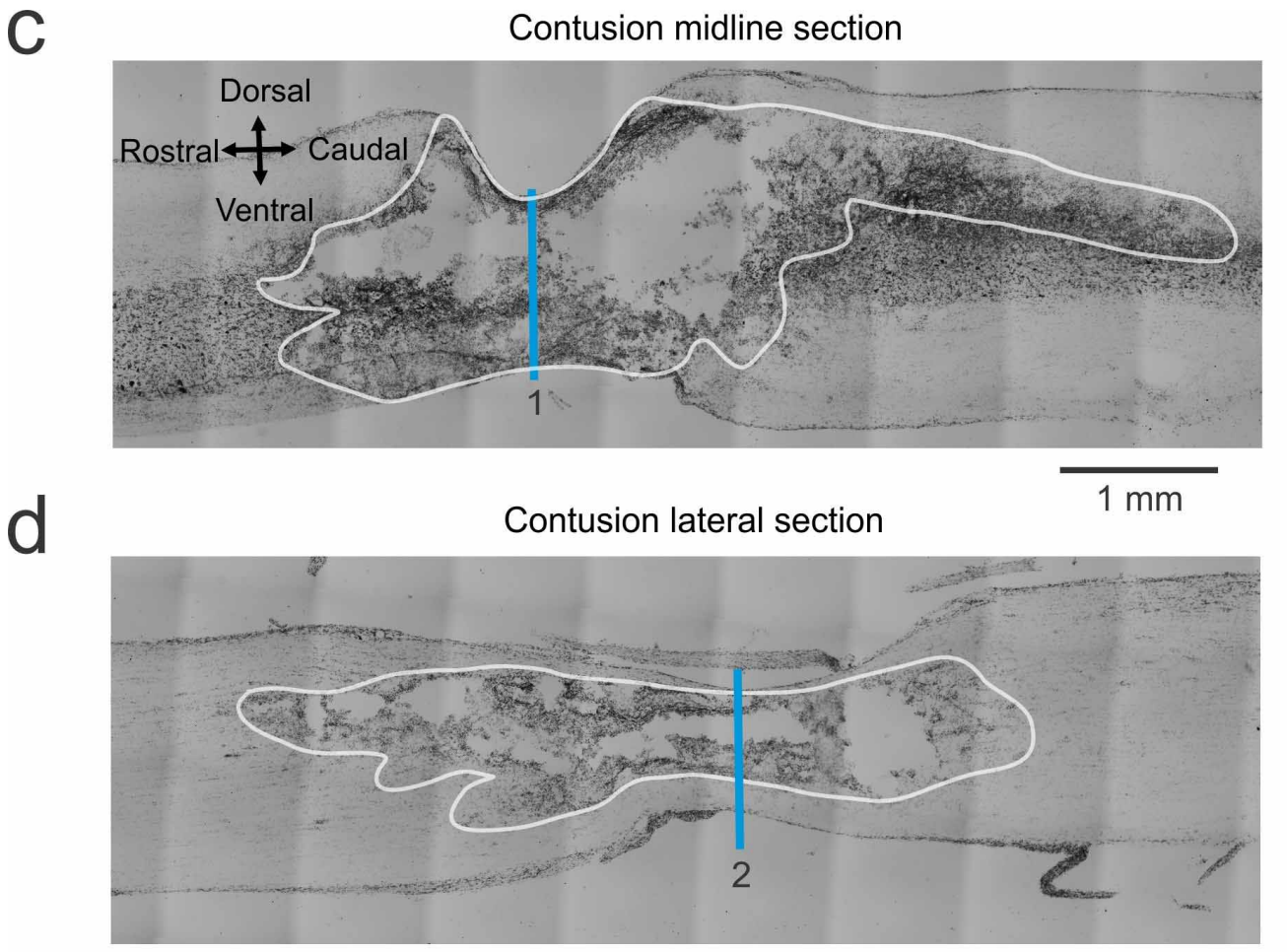
c
Contusion midline section
Dorsal
Rostral
Caudal
Ventral
1
1 mm
d
Contusion lateral section
2
e
White matter injury: 96%
1
2
f
White matter injury
(% of total uninjured)
100
50
0
Total
Dorsal
Ventral
g
Extent of injury (mm)
10
5
0

h

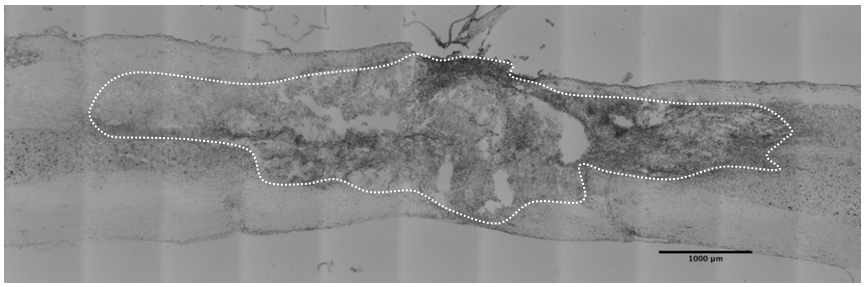

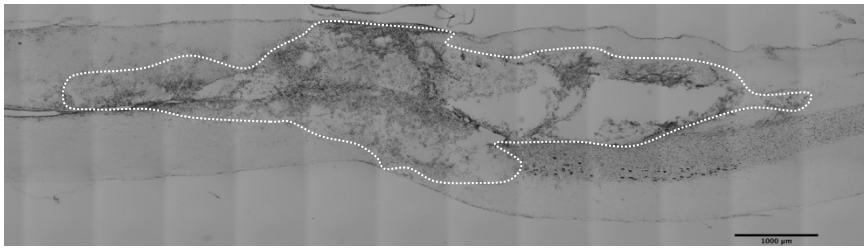

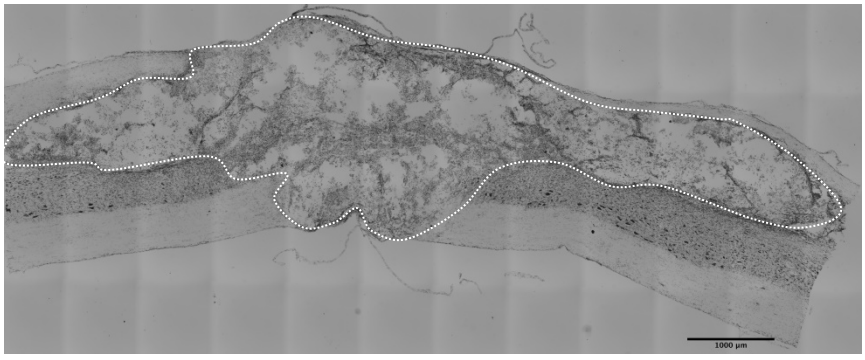

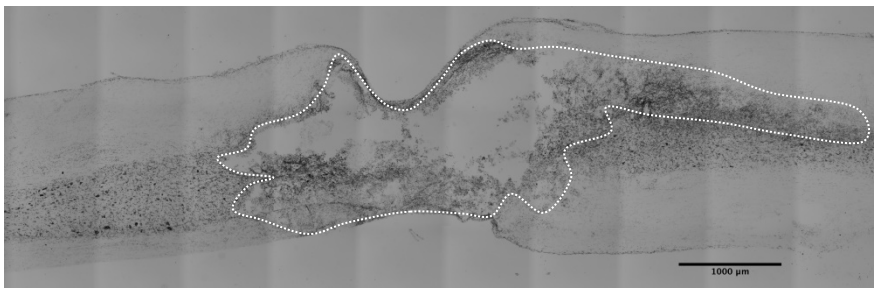

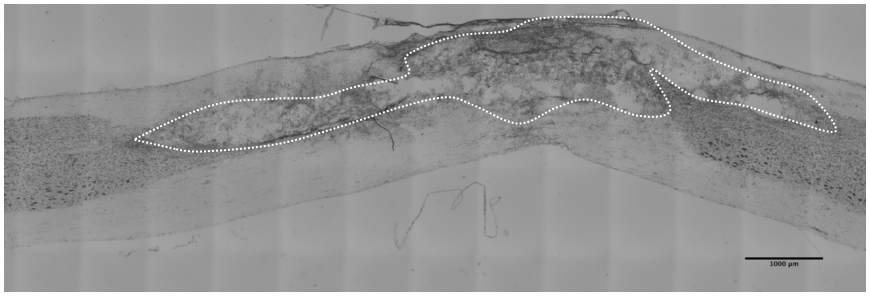

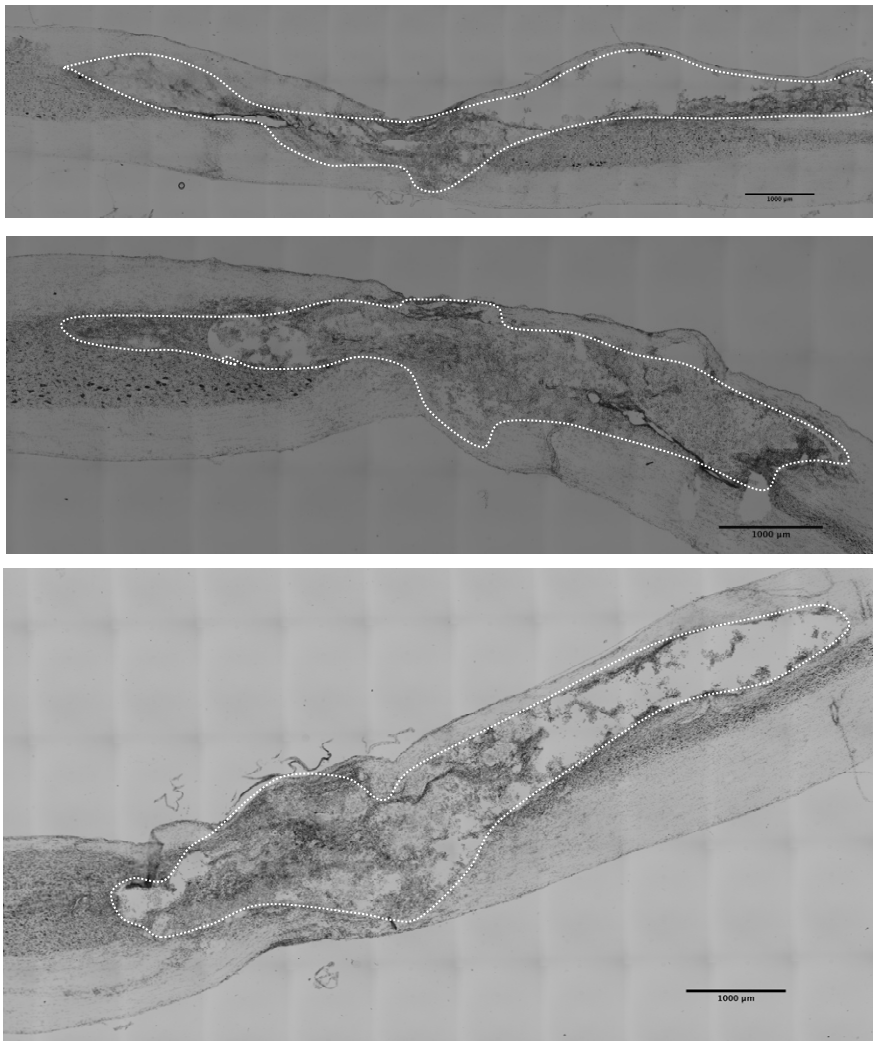

Supplementary Figure 16. Injury extent in rats used for studying locomotion. Staggered hemisections were used to eliminate descending axons, including 5-HT, to simplify the interpretation of the trace amine actions on 5-HT receptors, and severe contusions were used to eliminate most descending axons, but mimic a more clinical relevant injury. **(a)** Horizontal section through the thoracic cord of rat with a typical staggered hemisection (cresyl-violet counter stain). Lesions indicted at arrows, with the T10 hemisection performed first (deliberately over the midline) and then two weeks later the T7 hemisection performed on the opposite side. Serial reconstruction of the maximum extent of each lesion is indicated below, with the orange shading. **(b)** Overlay of these two hemisections, to demonstrate that when combined they interrupt all direct descending brain-derived axons. In particular, 5-HT fibers are eliminated, as we quantified previously in the lumbar cord far caudal to the injury[2,19]. Only propriospinal relay neurons (not 5-HT fibres) between these hemisections can bridge the lesion gap to initiate locomotion in the lumbar region[19]. **(c)** Contusion injury. Sagittal section through the thoracic spinal cord at T8 contusion injury site (midline section; maximum injury quantified at blue line). Damaged tissue circled with white line, showing no residual white matter (wm) in this section. **(d)** A more lateral sagittal section in the same rat, with some preserved wm, mostly ventral (quantified at epicentre, blue). **(e)** Schematic representation of injury (orange) and residual wm (white), constructed from sagittal sections (1, 2 from above), and overlaid over uninjured cord profile above the injury, with white regions corresponding to thickness of residual dorsal and ventral wm at the injury epicenter.

Scales same in c-e. **(f)** Quantification of mean wm damage in contused rats, computed as 100% minus the area of wm preserved at injury epicentre divided by total wm area in uninjured cord rostral to the injury (x100%; error bars, s.e.m; dots, individual rats). Computed for total wm, dorsal horn wm and ventral horn wm (ventral + dorsal = total). **(g)** Quantification of maximum rostral-caudal extent of injury. Overall, the white matter was injured by ~ 90%, consistent with our locomotor data variability, because a 90% injury is the threshold between good and poor locomotor recovery, especially with spared ventral tissue[20]. **(h)** Lesions in all rats with contusions of f-g; sagittal section for each rat, at maximal lesion extent.

Supplementary References

1. Crawford, J.H. & Rosenberger, H. Studies on human capillaries: II. Observations on the Capillary Circulation in Normal Subjects. *J Clin Invest* **2**, 351-364 (1926).
2. Li, Y.*, et al.* Synthesis, transport, and metabolism of serotonin formed from exogenously applied 5-HTP after spinal cord injury in rats. *J Neurophysiol* **111**, 145-163 (2014).
3. Ramos, D.*, et al.* The Use of Confocal Laser Microscopy to Analyze Mouse Retinal Blood Vessels. in *Confocal Laser Microscopy - Principles and Applications in Medicine, Biology, and the Food Sciences* (ed. Lagali, N.) (Intech, 2013).
4. Alliot, F., Rutin, J., Leenen, P.J. & Pessac, B. Pericytes and periendothelial cells of brain parenchyma vessels co-express aminopeptidase N, aminopeptidase A, and nestin. *J Neurosci Res* **58**, 367-378 (1999).
5. Cohen, Z.*, et al.* Multiple microvascular and astroglial 5-hydroxytryptamine receptor subtypes in human brain: molecular and pharmacologic characterization. *J Cereb Blood Flow Metab* **19**, 908-917 (1999).
6. Narzo, A.F.*, et al.* Decrease of mRNA Editing after Spinal Cord Injury is Caused by Down-regulation of ADAR2 that is Triggered by Inflammatory Response. *Sci Rep* **5**, 12615 (2015).
7. Winkler, E.A., Bell, R.D. & Zlokovic, B.V. Central nervous system pericytes in health and disease. *Nat Neurosci* **14**, 1398-1405 (2011).
8. Sieczkiewicz, G.J. & Herman, I.M. TGF-beta 1 signaling controls retinal pericyte contractile protein expression. *Microvasc Res* **66**, 190-196 (2003).
9. Ribatti, D., Nico, B. & Crivellato, E. The role of pericytes in angiogenesis. *Int J Dev Biol* **55**, 261-268 (2011).
10. van Doorn, R.*, et al.* Sphingosine 1-phosphate receptor 5 mediates the immune quiescence of the human brain endothelial barrier. *J Neuroinflammation* **9**, 133 (2012).
11. Chen, M.H.*, et al.* Influences of HIF-lalpha on Bax/Bcl-2 and VEGF expressions in rats with spinal cord injury. *Int J Clin Exp Pathol* **6**, 2312-2322 (2013).
12. Anders, S. & Huber, W. Differential expression analysis for sequence count data. *Genome Biol* **11**, R106 (2010).
13. Robinson, M.D. & Oshlack, A. A scaling normalization method for differential expression analysis of RNA-seq data. *Genome Biol* **11**, R25 (2010).
14. Hamilton, N.B., Attwell, D. & Hall, C.N. Pericyte-mediated regulation of capillary diameter: a component of neurovascular coupling in health and disease. *Front Neuroenergetics* **2**(2010).
15. Murray, K.C.*, et al.* Recovery of motoneuron and locomotor function after spinal cord injury depends on constitutive activity in 5-HT2C receptors. *Nat Med* **16**, 694-700 (2010).
16. Segreti, J.A., Polakowski, J.S., Blomme, E.A. & King, A.J. Simultaneous measurement of arterial and left ventricular pressure in conscious freely moving rats by telemetry. *J Pharmacol Toxicol Methods* **79**, 23-33 (2016).

17. Borowsky, B.*, et al.* Trace amines: identification of a family of mammalian G protein-coupled receptors. *Proc Natl Acad Sci U S A* **98**, 8966-8971 (2001).
18. Bunzow, J.R.*, et al.* Amphetamine, 3,4-methylenedioxymethamphetamine, lysergic acid diethylamide, and metabolites of the catecholamine neurotransmitters are agonists of a rat trace amine receptor. *Mol Pharmacol* **60**, 1181-1188 (2001).
19. Fouad, K.*, et al.* Locomotion after spinal cord injury depends on constitutive activity in serotonin receptors. *J Neurophysiol* **104**, 2975-2984 (2010).
20. Schucht, P., Raineteau, O., Schwab, M.E. & Fouad, K. Anatomical correlates of locomotor recovery following dorsal and ventral lesions of the rat spinal cord. *Exp Neurol* **176**, 143-153 (2002).